

J. Electroanal. Chem., 301 (1991) 77–85
Elsevier Sequoia S.A., Lausanne

An iridium based mercury ultramicroelectrode

Fabrication and characterization

Samuel P. Kounaves and Wen Deng

Department of Chemistry, Tufts University, Medford, MA 02155 (USA)

(Received 15 June 1990; in revised form 13 August 1990)

Abstract

A mercury ultramicroelectrode (Hg-UME) has been prepared by electrochemical deposition of mercury on an iridium substrate. The iridium UMEs can be prepared with radii of 1–20 μm using a molten salt etching solution of NaCl and NaNO₃. The Ir and Hg UMEs have been characterized by cyclic voltammetry and chronoamperometry, and microscopically, and are shown to exhibit diffusional behavior in accord with microelectrode theory and geometry. The mercury is well adhering and stable for long periods of time, with no indication of amalgam formation. The iridium based Hg-UME appears to be a stable and rugged mercury electrode with potential uses for *in situ* and *in vivo* electrochemical analysis.

INTRODUCTION

Ultramicroelectrodes (UME), typically less than 20 μm in size, have been shown to possess several unique characteristics in terms of such properties as transport rates, capacitive charging, and reduction in *iR* drop. In the past few years they have rapidly become invaluable in a wide range of research areas and applications [1]. As with larger electrodes, the most common materials used in their preparation are platinum, gold and carbon fiber. Platinum UMEs have been fabricated down to diameters as small as 0.003 μm and in various geometries such as disk [2,3], cylindrical [4]; and conical [5]. Typical carbon fiber electrodes have diameters in the range of 5–20 μm and are similarly used either as fibers of 1–5 μm length or as disks [6].

Because of its well known favorable electrochemical properties, mercury has been in practice one of the most widely used electrode materials. Development of

mercury UMEs would be of great value in extending these properties to the microelectrode domain. Attempts at fabricating mercury UMEs both on solid substrates and in bulk form have been made by several groups. Pons et al. [7] constructed a dropping mercury UME using a glass capillary tubing with a small mercury reservoir in the center. The mercury droplets are driven from the device by heating the capillary in a small oven. Even though the device performs well and does not suffer from any amalgamation problems associated with platinum based electrodes, it has many of the same problems that plague the classical DME or HMDE. In terms of plating mercury on a substrate to form a film or semisphere, Wehmeyer and Wightman [8] deposited Hg(I) onto a platinum disk with a radius as small as $0.3 \mu\text{m}$ and used it to demonstrate that anodic stripping voltammetry (ASV), with a quiescent solution during deposition, could be performed for lead in the concentration range of 7×10^{-7} to 1×10^{-10} M. Baranski [9] prepared mercury-film microelectrodes (7–10 μm diameter) by deposition of mercury on carbon fiber or platinum wire and used them for rapid voltammetric determinations of trace metals in very small samples.

As with larger electrodes, the dissolution of a substrate such as Pt, Au or Ag in mercury and the resulting formation of intermetallic compounds with analyte metals deposited into the film, can limit the utility of such electrodes severely [9]. This is especially true in studies utilizing anodic stripping voltammetry (ASV) or in fundamental electrochemistry where only mercury electrodes are suitable. It has been suggested that a substrate that is totally inert with respect to mercury would be preferable for constructing such an electrode. However, similarly to previous experiences with macro-electrodes [10], totally inert substrates such as glassy carbon give bad reproducibility in the deposition process and have usually resulted in a failure of the mercury drop to adhere to the carbon [7].

About five years ago an attempt was made to find a more suitable substrate on which to deposit mercury [11]. Using data from both theoretical calculations and experimental studies, it was shown that iridium was a viable substrate for the formation of a mercury film or hemisphere [12,13]. This noble metal possesses two properties which make it ideal for this use: (1) its solubility in mercury is well below $10^{-6}\%$ by weight [12,14]; (2) mercury can be electroplated onto an iridium disk (1–4 mm dia.) in such a way as to give a uniform film or hemispherical coverage [13]. In addition, studies have shown that the iridium-based mercury film electrode behaves according to thin film theory and can be used reliably for analysis [15,16]. Because iridium wire of less than $127 \mu\text{m}$ in diameter is not commercially available (due to the difficulties in drawing iridium to smaller diameters), the only reported attempts at fabricating an iridium based mercury UME have been made using this diameter iridium wire [16–18]. However, because of its size, and with the time scale used, the characteristics observed were those of neither a *micro-* nor a *macro-* electrode. No attempts at fabricating iridium UMEs of less than $127 \mu\text{m}$ have been recorded in the literature to date. We report here the fabrication and preliminary characterization of a micrometer sized iridium based mercury UME.

EXPERIMENTAL

Reagents

All solutions were prepared with 18 M Ω cm water from a Barnstead Nanopure system. A.C.S. Reagent grade $K_3Fe(CN)_6$, $Ru(NH_3)_6Cl_3$, KNO_3 , $HClO_4$, $Hg_2(NO_3)_2$, $NaNO_3$, $NaCl$, and iridium wire (150 μ m diameter, 99.9% pure) all from Aldrich, were used as received. Alumina for electrode polishing was from Buehler.

Apparatus

Cyclic voltammetry and chronoamperometry were performed using either an EG&G PAR Model 273 potentiostat/galvanostat interfaced to an IBM PS/2-30 with custom software, or a CYSY-1B Electroanalysis System (Cypress Systems) also interfaced to an IBM PS/s-30. The voltage for the etching process was supplied by Model 3017A function generator (BK Precision). All voltammetric experiments were performed using a three electrode system consisting of the working electrode, a platinum counter electrode and a sodium saturated calomel reference (SSCE). The heater for the molten salt etching bath was a custom-made fiberglass fabric heating mantle (Glas-Col). Optical *in situ* microscopic observations of the electrodes were made with a Metaval-H (Leco/Jena) inverted microscope.

Tip etching

The electrochemical etching was carried out in a molten salt bath composed of $NaNO_3$ and $NaCl$ in a 20 mL platinum crucible. Since both the ratio of $NaNO_3$ to $NaCl$ and the applied potential waveform have an effect on the melting temperature, the etching rate, and the final geometry of the tip, various combinations of mixture ratios and potential waveforms were tried.

Square waveform potentials gave a smoother surface and a more radially homogeneous geometry, but the etching time was of the order of 8–10 h. Sine wave potentials made it somewhat more difficult to control the geometry and smoothness, but required only 6–15 min for complete etching. Waveform frequency also plays an important role. Lower frequencies took less time but gave a rougher surface, while higher frequencies took longer but produced a smoother surface. Using a mixture of 4 : 1 ($NaNO_3$: $NaCl$) at 520 °C (the maximum for our heating mantle) required an etching time of about 5–6 min (using 100 Hz sine wave). Increasing the ratio to 8 : 1 decreased the melting temperature to 390 °C but increased the electrolysis time to about 20 min.

The optimum conditions were found to be a 6 : 1 ($NaNO_3$: $NaCl$) salt mixture at 445 °C with a 100 Hz sine-wave at 1.0 V (rms), applied between the immersed Ir wire and the Pt crucible. The etching was performed by immersing an Ir wire approximately 5–6 cm long to a depth of about 3 mm or until the current was about 100 mA rms. The current was monitored during the entire etching process. After a 9–10 min decline to a current of about 50–60 mA, the current dropped abruptly to almost zero. At that point, the Ir wire was withdrawn from the melt. Removing the

wire before the current dropped or at times greater than 10–20 s after the drop resulted in tips of unsuitable structure.

Several other etching methods were attempted, including aqueous solutions of KCN, and mixtures of HCl + H₂SO₄; however, none of them produced acceptable results as easily. If a dc potential was used in place of the sine wave, a dark passivating layer would form on the electrode and hinder further etching. Only on reversing the polarity of the applied potential on the electrode and platinum crucible could the coating be removed and the etching resumed.

Electrode assembly

The etched Ir wire was placed into a 0.1 mm i.d. (1 μ L) glass capillary pipette (Drummond Scientific) and the etched end sealed into the capillary by melting the glass to about 1 mm from the tip. The other end of the Ir wire was twisted around a solid copper wire and brazed at 600 °C using silver alloy and a microflame gas torch (Microflame). The entire assembly, except for several millimeters at the tip, was made rigid by covering with heat shrinkable tubing. The tip was then ground flat using a high speed rotating wheel with 600 grit and 1200 grit silicon carbide (Carbimet[®], Buehler), and hand polished successively with 1.0, 0.3, and 0.05 μ m alumina (Micropolish[®], Buehler). The completed iridium UME, shown diagrammatically in Fig. 1, could then be used directly, or as a substrate for the deposition of the mercury. Microscopic examination showed the surface to be defect free and the glass seal around the wire to be complete.

Mercury film / hemisphere deposition

The mercury hemisphere on the Ir substrate was formed by coulometric deposition at -0.4 V vs. SSCE in a deoxygenated solution containing 10 mM Hg(I) and 0.1 M HClO₄. Deposition efficiencies ranged from 85 to 90%. The thickness used for each electrode is given below. For thinner Hg layers a previously described procedure was used [13].

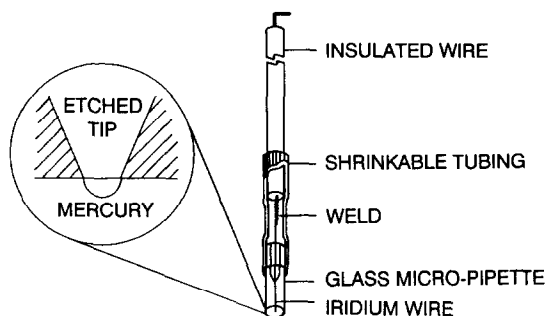


Fig. 1. Diagram of the iridium based ultramicroelectrode. The tip may be etched anywhere from 20 μ m to less than 1 μ m at its smallest point and used with or without a mercury layer.

RESULTS AND DISCUSSION

Electrochemical characterizations of the Ir-UME and Hg-UME were performed using cyclic voltammetry and chronoamperometry. In addition, these techniques allow for confirmation of both proper sealing between glass and iridium, and estimated surface area size.

Characterization of the Ir-UME

Figure 2 shows the cyclic voltammograms for the reduction of 6 mM $\text{K}_3\text{Fe}(\text{CN})_6$ in 1 M KNO_3 aqueous solution at a bare Ir-UME electrode with a microscopically measured radius of 20 μm . The scan rate for the six curves varies from 2 to 500 mV/s. For scan rates of 2 and 10 mV/s the shape of the voltammograms is sigmoidal, with no oxidation current present. These features indicate that radial diffusion was established and that steady-state conditions were reached. At scan rates between 10 and 20 mV/s an oxidation current becomes evident. At scan rates ≥ 100 mV/s both forward and reverse scans develop peaks and a significant oxidation current becomes evident. The relationship for the limiting steady-state current at a UME,

$$i_L = anFDcr \quad (1)$$

where r is the electrode radius, $a = 4$ for a disk, and all other symbols have their usual meaning [ref. 1, p. 283], can be evaluated to determine the radius of the UME. Using the limiting current of $i_L = 79$ nA obtained from either the 2 or 5 mV/s scan

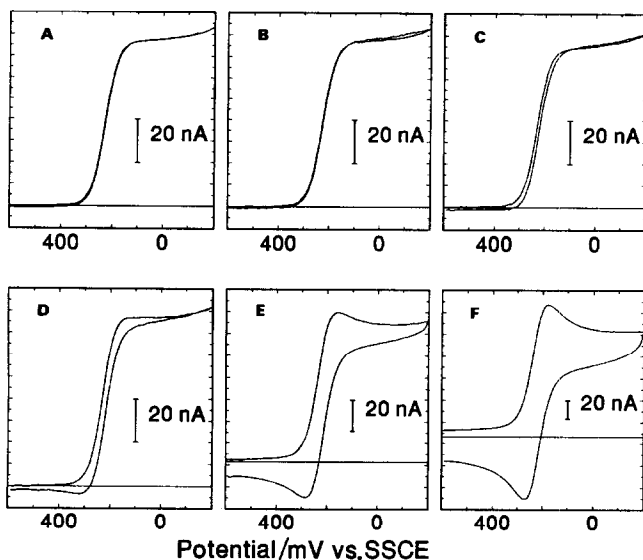


Fig. 2. Cyclic voltammograms for the Ir-UME using 6 mM $\text{K}_3\text{Fe}(\text{CN})_6$ in 1 M KNO_3 at potential scan rates of (A) 2, (B) 5, (C) 10, (D) 20, (E) 100, and (F) 500 mV/s. Zero current indicated by horizontal line.

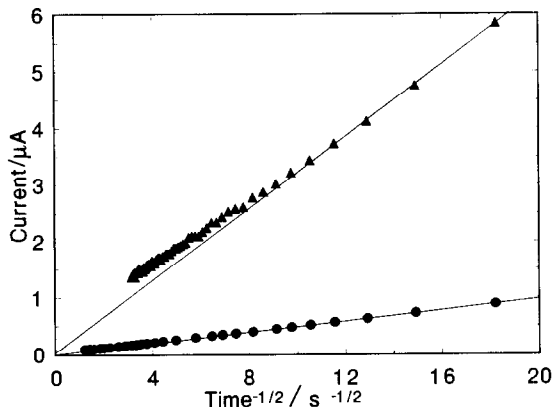


Fig. 3. Current vs. $1/t^{1/2}$ plots for the $21 \mu\text{m}$ Ir-UME in $6 \text{ mM K}_3\text{Fe}(\text{CN})_6 + 1 \text{ M KNO}_3$ (●), and for Hg-UME on the same substrate in $5 \text{ mM Ru}(\text{NH}_3)_6\text{Cl}_3 + 0.1 \text{ M KH}_2\text{PO}_4 + \text{NaOH pH} = 7$ buffer solution (▲).

(Fig. 3) and $D = 7.84 \times 10^{-6} \text{ cm}^2/\text{s}$ [19] yields a radius for this UME of $r = 21 \mu\text{m}$, in good agreement with the optical measurement.

We can also evaluate the electrochemical behavior quantitatively and estimate the electrode area of the Ir-UME independently by the use of the Cottrell equation,

$$i = nFAD^{1/2}c/(\pi^{1/2}t^{1/2}) \quad (2)$$

where all symbols have their usual meaning.

If we assume that the Ir-UME is a flat disk and that linear diffusion occurs, then a plot of i vs. $1/t^{1/2}$ should give a linear relationship at short times. As linear diffusion changes to hemispherical diffusion the linear relationship will not hold and a deviation to higher current will occur. Fig. 3 (●) shows the i vs. $1/t^{1/2}$ data for the $r = 21 \mu\text{m}$ UME in $6 \text{ mM K}_3\text{Fe}(\text{CN})_6 + 1 \text{ M KNO}_3$. The potential was stepped from 500 mV to 0 mV (vs. SSCE) and the current data taken for 1000 ms . The fit of the data to the Cottrell equation for the first 100 ms is excellent with a correlation coefficient = 0.99 . The transition to hemispherical diffusion starts to become evident at around $5 \text{ s}^{-1/2}$. Using the slope of the i vs. $1/t^{1/2}$ data in eqn. (2) the electrode area was calculated to be $1.8 \times 10^{-6} \text{ cm}^2$, resulting in $r = 23 \mu\text{m}$. From the data shown above and for several other UMEs tested, the results indicate that the fabrication procedure results in proper sealing between the glass and the iridium wire, and that electrochemical and physical surface area are equivalent.

Characterization of the Ir / Hg-UME

As previously pointed out, the shape of the deposited mercury can be varied from a thin film to almost a sphere [15,18] depending on the deposition parameters. Because of the intended use of these electrodes and the desire for ruggedness and stability, the hemispherical geometry was used the most and has been characterized the best. The thin-film is very rugged, but does not allow for any substantial

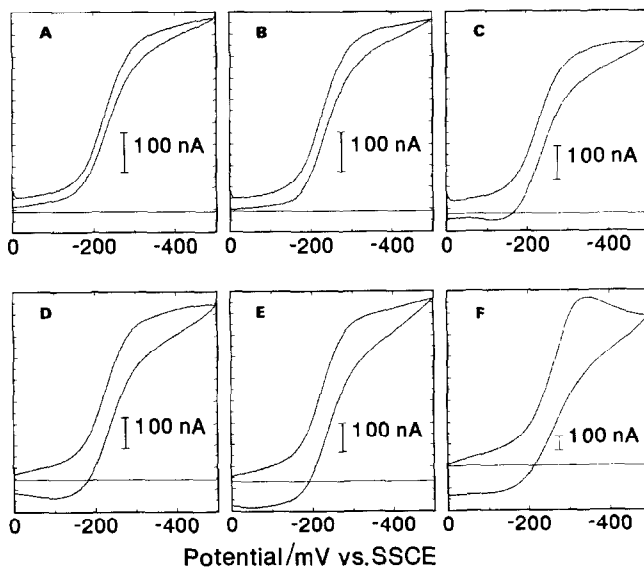


Fig. 4. Cyclic voltammograms for a hemispherical Hg-UME using 5 mM $\text{Ru}(\text{NH}_3)_6\text{Cl}_3$ in 0.1 M $\text{KH}_2\text{PO}_4 + \text{NaOH}$ pH = 7 buffer solution at potential scan rates of (A) 2, (B) 5, (C) 10, (D) 20, (E) 100, and (F) 500 mV/s. Zero current indicated by horizontal line.

concentration of analyte metals in such techniques as ASV. On the other hand, the larger almost spherical geometry has less preconcentration problems in ASV, but is not mechanically very stable. The deposition of mercury at this electrode was found to follow the behavior expected for spherical diffusion to a growing mercury hemisphere, with the deposition current being linearly proportional to $t^{1/2}$ [20]. As with previous studies [8,13,18], the deposition charge could be used directly and reproducibly to determine coverage of the substrate. Typically, for an electrode with $r = 20 \mu\text{m}$, a deposition time of about 800 s would result in a hemispherical coverage.

A quantitative estimation of the geometry of the mercury can be obtained from considering the equation for the diffusion limited current. Depending on whether the UME is a disk, hemisphere or sphere, the value of a in eqn. (2) will be 4, 2π , or 4π , respectively. Using these results in conjunction with the radius calculated from the known deposition time serves as a complementary check on the size and geometry of the Hg-UME. Figure 4 shows the cyclic voltammograms for the reduction of 5 mM $\text{Ru}(\text{NH}_3)_6\text{Cl}_3$ in a 0.1 M $\text{KH}_2\text{PO}_4 + \text{NaOH}$ pH = 7 buffer solution at a Hg hemisphere formed on an Ir-UME electrode with a microscopically measured radius of $20 \mu\text{m}$. The scan rate for the six curves varies from 2 to 500 mV/s. For scan rates of 2 and 10 mV/s the shapes of the voltammograms are sigmoidal, with no oxidation current present. At scan rates between 10 and 20 mV/s an oxidation current becomes evident. At scan rates ≥ 100 mV/s both forward and reverse scans develop peaks and an oxidation current becomes evident.

Using the limiting current of $i_L = 390$ nA obtained from either the 2 or 5 mV/s scan (Fig. 4) and $D = 6.00 \times 10^{-6}$ cm²/s [8] yields an apparent radius for this UME of $r = 35$ μ m. The chronoamperometric curve for this electrode is shown in Fig. 3 (\blacktriangle). Unlike the results for the disk Ir-UME the hemispherical shape of the Hg-UME shows the earlier deviation from linear to spherical diffusion. Using the slope of the i vs. $1/t^{1/2}$ data in eqn. (2) the electrode area was calculated to be 3.24×10^{-6} cm², resulting in an apparent $r = 32$ μ m. The excellent agreement between these data, with the assumption of $a = 2\pi$, and the presumed Hg shape from the deposition data, indicates that the deposition of the Hg does indeed occur in a hemispherical shape.

CONCLUSIONS

The iridium-based mercury UME has been characterized by optical microscopy, cyclic voltammetry, and chronoamperometry, and has been shown to exhibit microelectrode behavior. The mercury is well adhering and stable for long periods of time, with no indication of amalgam formation. The iridium based mercury ultramicroelectrode appears to be a stable and rugged mercury electrode with potential uses for *in situ* and *in vivo* electrochemical analysis.

Because of the unique properties of the mercury UME, it could be used in analyses with sample volumes in the microliter range, without stirring of the solution, and without deoxygenation. Recently, by applying the technique of square wave anodic stripping voltammetry with very short or no predeposition time of the metal into the mercury, these mercury UMEs have been used to determine lead at concentrations of 10^{-4} down to 10^{-9} M [21].

REFERENCES

- 1 R.M. Wightman and D.O. Wipf, in A.J. Bard (Ed.), *Electroanalytical Chemistry*, Vol. 15, Marcel Dekker, New York, 1989, pp. 267–353.
- 2 K. Itaya, T. Abe and I. Uchida, *J. Electrochem. Soc.*, 134 (1987) 1191.
- 3 P.D. Pendley and H.D. Abruña, *Anal. Chem.*, 62 (1990) 782.
- 4 S.T. Singleton, J.J. O'Dea and J. Osteryoung, *Anal. Chem.*, 61 (1989) 1211.
- 5 R.M. Penner, M.J. Heben and N.S. Lewis, *Anal. Chem.*, 61 (1989) 1630.
- 6 R.M. Wightman, *Science*, 240 (1988) 415.
- 7 J.W. Pons, J. Daschbach, S. Pons and M. Fleischmann, *J. Electroanal. Chem.*, 239 (1988) 427.
- 8 K.R. Wehmeyer and R.M. Wightman, *Anal. Chem.*, 57 (1985) 1989.
- 9 A.S. Baranski, *Anal. Chem.*, 59 (1987) 662.
- 10 M. Stulikova, *J. Electroanal. Chem.*, 48 (1983) 33.
- 11 S.P. Kounaves, Ph.D. Thesis, University of Geneva, Switzerland, 1985; University Microfilms International, Ann Arbor, MI, 86-18608.
- 12 S.P. Kounaves and J. Buffle, *J. Electrochem. Soc.*, 133 (1986) 2495.
- 13 S.P. Kounaves and J. Buffle, *J. Electroanal. Chem.*, 216 (1987) 53.
- 14 C. Guminski, Z. Galus and C. Hirayama (Eds.), *Solubility Data Series—Metals in Mercury*, Pergamon Press, Oxford, 1986.
- 15 S.P. Kounaves and J. Buffle, *J. Electroanal. Chem.*, 239 (1988) 113.
- 16 C. Wechter and J. Osteryoung, *Anal. Chem.*, 61 (1989) 2092.

- 17 J. Golas, Z. Galus and J. Osteryoung, *Anal. Chem.*, 59 (1987) 389.
- 18 J. Golas and Z. Kowalski, *Anal. Chim. Acta*, 221 (1989) 305.
- 19 M. Kakihana, H. Ikeuchi, G.P. Sato and K. Tokudo, *J. Electroanal. Chem.*, 108 (1980) 381.
- 20 B. Scharifker and G. Hills, *J. Electroanal. Chem.*, 130 (1981) 81.
- 21 S.P. Kounaves and W. Deng, *Anal. Chem.*, submitted.